Supporting Information

Text S1 Procedure of MENs construction

To illuminate the effect of salinity on the microbial interaction, four MENs were constructed using the online MENA pipeline by following these steps (Tu et al., 2015; Deng et al., 2016). First, OTUs detected in less than four samples would be removed to eliminate low-frequency OTUs, and the relative abundance of individual OTUs was used to construct an abundance matrix, which is standardized as the standardized data matrix and used for subsequent correlation analysis. And pairwise Pearson correlation coefficients are used to construct a Pearson correlation matrix. Second, the correlation matrix was transformed into a similarity matrix by taking the absolute value of correlation matrix to define the abundance similarity between OTUs across different samples. Third, the adjacency matrix is derived from the OTU abundance similarity matrix by applying an appropriate threshold, S_t, which was defined using the RMT-based network method (Luo et al., 2006; Luo et al., 2007). In this study, we choose the St by testing with decreasing the cutoff from the top, and finally 0.92 was selected as the appropriate threshold of four networks. Fourth, modules were detected by the fast-greedy modularity optimization, and then the modularity value (M) was calculated as previously described (Clauset et al., 2004; Zhou et al., 2010).

For network comparison, Maslov-Sneppen procedure was explored to construct the random networks corresponding to all experimental networks (Maslov and Sneppen, 2002). For each network, a total of 100 randomly rewired networks were constructed and all of the network indexes were calculated individually. Then, the average and standard deviation for each index of all of the random networks were obtained. A standard t test was employed to determine the significance of network indexes. $P < 0.05$ was the criteria of statistically significant difference.

Text S2 Procedure of iDIRECT

iDIRECT was applied to separate direct and indirect relationships in each MEN and focused on the direct associations in the network. Based on the basic algorithms, the total association between two nodes *i* and *j* (G_{ij}) is the sum (using $\oplus$, Eq. (1)) of their direct association (S_{ij}) and indirect association. iDIRECT does not explicitly use $\boldsymbol{G}^{-1}$ in the formulation, The formulation starts from dividing the whole system into small subsystems. For a given node *i*, first, we select two of *i*'s neighbors, *j* and *k*, and calculate the transitivity matrix $T_{i,jk}$ by solving Eq. (2). The nonlinear system in Eq. (2) was solved by T-solver, using $\boldsymbol{G}$ to compute $\boldsymbol{T}_i$.

$$u \oplus v = \frac{u+v-2uv}{1-uv}, \quad (1)$$

$$\begin{cases} G_{kj} = T_{i,kj} \oplus \left(T_{j,ki} T_{k,ij}\right); \\ G_{ki} = T_{j,ki} \oplus \left(T_{k,ij} T_{i,kj}\right); \\ G_{ij} = T_{k,ij} \oplus \left(T_{i,kj} T_{j,ki}\right), \end{cases} \quad (2)$$

The transitivity matrix ($\boldsymbol{T}_i$) was then introduced to eliminate all self-looping-induced indirect paths. Its (*i*,*k*,*j*)-th component, $\boldsymbol{T_{i,kj}}$ is the association strength between node $\boldsymbol{k}$ and $\boldsymbol{j}$, excluding paths passing $\boldsymbol{i}$. $\boldsymbol{S_{ik}}$ is the direct association strength between node *i* and *k*. Therefore, the indirect association through $\boldsymbol{k}$ is $\boldsymbol{S_{ik}} \oplus \boldsymbol{T_{i,kj}} = \boldsymbol{S_{ik}}\boldsymbol{T_{i,kj}}$, which contains no self-looping indirect paths,

because we explicitly exclude them in the definition of $T_{i,kj}$. Combining the results above, we calculate the total association G_{ij} from S_{ij} and $T_{i,kj}$ by Eq. (3). Iterating j over all i's neighbors will give us all the equations we need to solve all the direct association strength S_{ij} (collectively as a matrix **S**) from G_{ij} (collectively as a matrix $\boldsymbol{G}$) and $T_{i,kj}$ (collectively as $\boldsymbol{T}i$). Here, the nonlinear system in Eq. (4) was solved by S-solver, using $\boldsymbol{G}$ and $\boldsymbol{T}_i$ to compute $\boldsymbol{S}$. Therefore, Eq. (3) and its derived forms are the foundation of iDIRECT. In brief, iDIRECT accepts the observable total association matrix $\boldsymbol{G}$ as input and returns the direct association matrix $\boldsymbol{S}$ as output.

$$G_{ij} = S_{ij} \oplus S_{ik_2}T_{i,k_2j} \oplus S_{ik_3}T_{i,k_3j} \oplus \cdots \oplus S_{ik_d}T_{i,k_dj} \quad , \qquad (3)$$

$$\begin{bmatrix} G_{ik_1} \\ G_{ik_2} \\ \vdots \\ G_{ik_d} \end{bmatrix} = \begin{bmatrix} S_{ik_1} \\ S_{ik_2} \\ \vdots \\ S_{ik_d} \end{bmatrix} \oplus \left(\begin{bmatrix} 1 & T_{i,k_1k_2} & \cdots & T_{i,k_1k_d} \\ T_{i,k_2k_1} & 1 & \cdots & T_{i,k_2k_d} \\ \vdots & \vdots & \ddots & \vdots \\ T_{i,k_dk_1} & T_{i,k_dk_2} & \cdots & 1 \end{bmatrix} \otimes \begin{bmatrix} S_{ik_1} \\ S_{ik_2} \\ \vdots \\ S_{ik_d} \end{bmatrix} \right)$$

$$\Longrightarrow G_i = S_i \oplus (T_i \otimes S_i), \quad , \qquad (4)$$

Table S1 Topological features of original and iDIRECT-processed networks.

(a) original networks

Datasets	No. of original OTUs	Similarity threshold (S_t)	Empirical networks							Random networks		
			Nodes	Links	R^2 of power law	Avg degree (avgK)	Average path distance (GD)	Avg clustering coefficient (avgCC)	Modularity (No. of modules)	Average path distance ± SD	Avg clustering coefficient ±SD	Modularity
0%	839	0.92	437	768	0.898	3.515	5.843	0.155	0.802 (49)	4.388 ± 0.055	0.015 ± 0.004	0.553 ± 0.006
1%	796	0.92	305	371	0.849	2.433	7.107	0.108	0.854 (58)	5.251 ± 0.130	0.009 ± 0.004	0.710 ±0.008
2%	697	0.92	227	433	0.841	3.815	5.082	0.195	0.736 (28)	3.779 ± 0.069	0.036 ± 0.008	0.494 ± 0.008
3%	492	0.92	127	183	0.835	2.882	4.83	0.155	0.748 (20)	4.149 ± 0.130	0.027 ± 0.012	0.585 ± 0.012

(b) iDIRECT-processed networks

Datasets	No. of original OTUs	Similarity threshold (S_t)	Empirical networks							Random networks		
			Nodes	Links	R^2 of power law	Avg degree (avgK)	Average path distance (GD)	Avg clustering coefficient (avgCC)	Modularity (No. of modules)	Average path distance ± SD	Avg clustering coefficient ±SD	Modularity
0%	839	0.92	407	590	0.923	2.899	8.037	0.098	0.837 (55)	4.843 ± 0.082	0.011 ± 0.004	0.635 ± 0.008
1%	796	0.92	260	287	0.961	2.208	7.769	0.066	0.894 (47)	5.745 ± 0.226	0.007 ± 0.004	0.757 ±0.009
2%	697	0.92	196	299	0.839	3.051	5.759	0.108	0.782 (33)	4.119 ± 0.104	0.027 ± 0.009	0.576 ± 0.009
3%	492	0.92	102	112	0.802	3.006	6.183	0.147	0.786 (22)	4.755 ± 0.262	0.016 ± 0.011	0.695 ± 0.015

Table S2 Putative keystone taxa detected in the association networks. RA means the relative abundance (%) of OTUs in microbial community.

(a) Module hubs

Network	OTUs	RA (%)	phylum	class	order	family	genus
0%	OTU28	1.106	Proteobacteria	Alphaproteobacteria	Rhodospirillales	Rhodospirillaceae	Defluviicoccus
	OTU1075	0.209	Proteobacteria	Betaproteobacteria	Rhodocyclales	Rhodocyclaceae	Thauera
	OTU599	0.303	Acidobacteria	Acidobacteria	Blastocatellales	Blastocatellaceae__Subgroup_4	norank
	OTU955	1.788	Proteobacteria	Gammaproteobacteria	Xanthomonadales	Xanthomonadales_Incertae_Sedis	Candidatus_Competibacter
	OTU198	0.021	Chloroflexi	Thermomicrobia	JG30-KF-CM45	norank_o__JG30-KF-CM45	norank_o__JG30-KF-CM45
	OTU581	0.311	Proteobacteria	Alphaproteobacteria	Rhodospirillales	Rhodospirillaceae	Defluviicoccus
	OTU663	0.352	Proteobacteria	Alphaproteobacteria	Rhodospirillales	Rhodospirillaceae	Defluviicoccus
	OTU43	0.164	Proteobacteria	Alphaproteobacteria	Rhodospirillales	unclassified_o__Rhodospirillales	unclassified_o__Rhodospirillales
	OTU629	0.026	Proteobacteria	Betaproteobacteria	SC-I-84	norank_o__SC-I-84	norank_o__SC-I-84
	OTU601	0.220	Proteobacteria	Alphaproteobacteria	Rhodobacterales	Rhodobacteraceae	unclassified_f__Rhodobacteraceae
	OTU577	0.170	unclassified	unclassified	unclassified	unclassified	unclassified
	OTU117	0.008	Acidobacteria	Acidobacteria	norank_c__Acidobacteria	norank_c__Acidobacteria	norank_c__Acidobacteria
	OTU736	0.237	Chloroflexi	Caldilineae	Caldilineales	Caldilineaceae	norank_f__Caldilineaceae
	OTU259	0.049	Acidobacteria	Acidobacteria	Subgroup_10	CA002	norank_f__CA002
	OTU750	0.029	Gemmatimonadetes	Gemmatimonadetes	Gemmatimonadales	Gemmatimonadaceae	norank_f__Gemmatimonadaceae
1%	OTU252	0.029	Chloroflexi	Caldilineae	Caldilineales	Caldilineaceae	norank_f__Caldilineaceae
	OTU771	0.334	Proteobacteria	Alphaproteobacteria	Rhodobacterales	Rhodobacteraceae	Gemmobacter
	OTU736	0.141	Chloroflexi	Caldilineae	Caldilineales	Caldilineaceae	norank_f__Caldilineaceae
	OTU793	0.752	Chloroflexi	Anaerolineae	Anaerolineales	Anaerolineaceae	norank_f__Anaerolineaceae
2%	OTU744	0.032	Chloroflexi	Anaerolineae	Anaerolineales	Anaerolineaceae	norank_f__Anaerolineaceae
	OTU771	0.282	Proteobacteria	Alphaproteobacteria	Rhodobacterales	Rhodobacteraceae	Gemmobacter
	OTU28	0.071	Proteobacteria	Alphaproteobacteria	Rhodospirillales	Rhodospirillaceae	Defluviicoccus
3%							

(b) Connectors

Network	OTUs	RA (%)	phylum	class	order	family	genus
0%	OTU555	0.021	Ignavibacteriae	Ignavibacteria	Ignavibacteriales	unclassified	unclassified
	OTU704	0.024	Chloroflexi	Caldilineae	Caldilineales	Caldilineaceae	norank_f__Caldilineaceae
	OTU635	0.126	Proteobacteria	Gammaproteobacteria	Xanthomonadales	Xanthomonadales_Incertae_Sedis	Candidatus_Competibacter
	OTU898	0.009	Proteobacteria	Gammaproteobacteria	Xanthomonadales	Xanthomonadaceae	Pseudoxanthomonas
1%							
2%	OTU380	0.368	Bacteroidetes	Cytophagia	Cytophagales	Cytophagaceae	norank_f__Cytophagaceae
	OTU1005	0.068	Proteobacteria	Betaproteobacteria	Rhodocyclales	Rhodocyclaceae	Azoarcus
3%							

(c) Network hub

Network	OTUs	RA (%)	phylum	class	order	family	genus
2%	OTU959	0.535	Bacteroidetes	Flavobacteriia	Flavobacteriales	Cryomorphaceae	norank_f__Cryomorphaceae

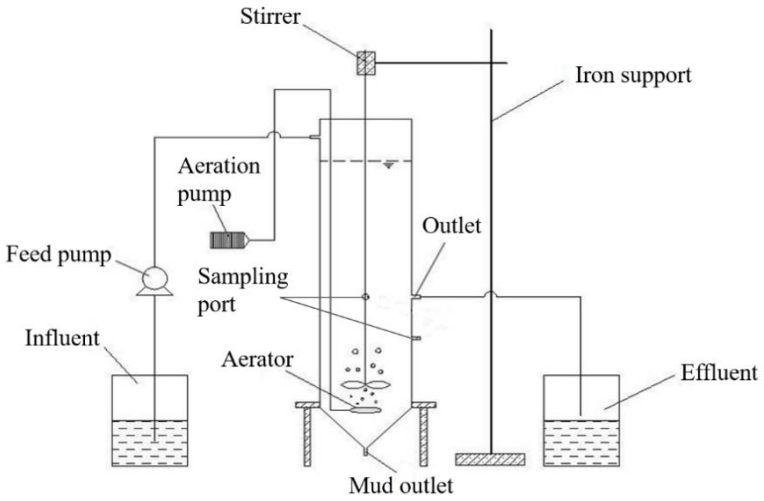

Fig. S1 Schematic diagram of the SBR system.

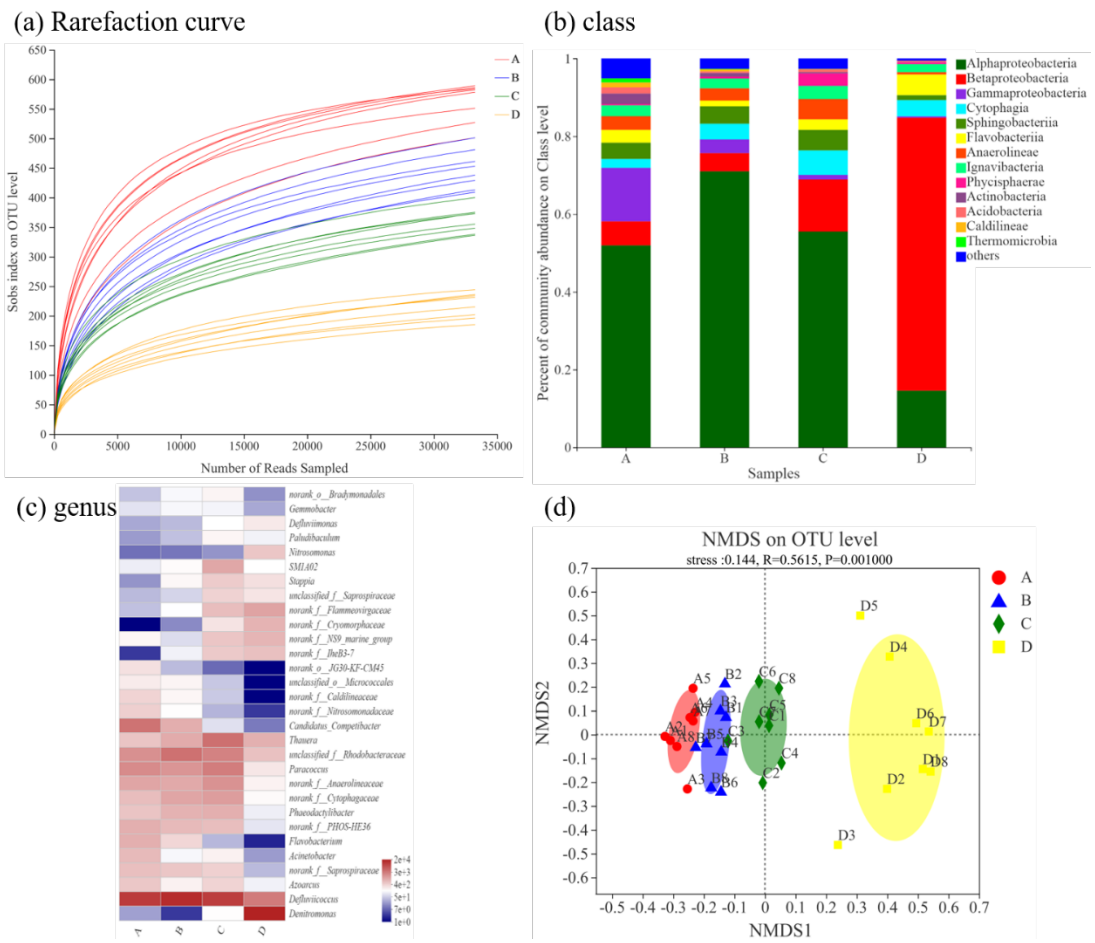

Fig. S2 Variation of microbial community composition in activated sludge system under elevated salinity. The rarefaction curve of 32 samples (a); and the fluctuation of major class (b) and genera (c); and the variation of microbial communities showed by NMDS (d) changed with elevated salinity.

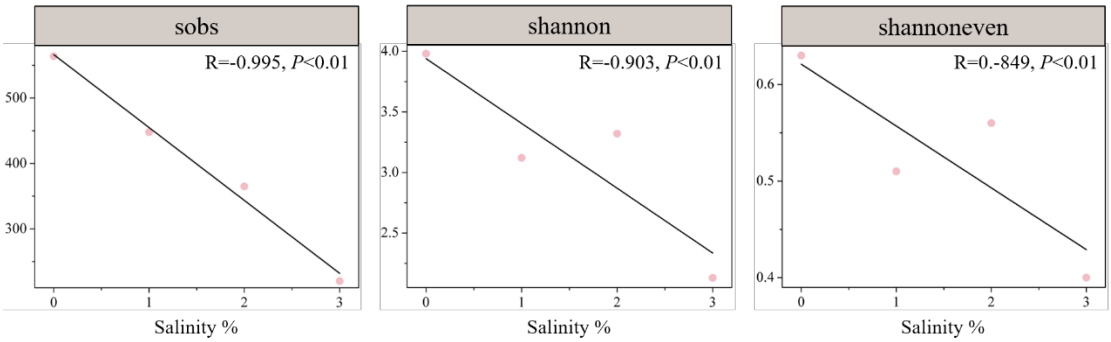

Fig. S3 Correlations between α-diversity indices of bacterial communities and salinity. Correlation values (R) and *P* values are labeled.

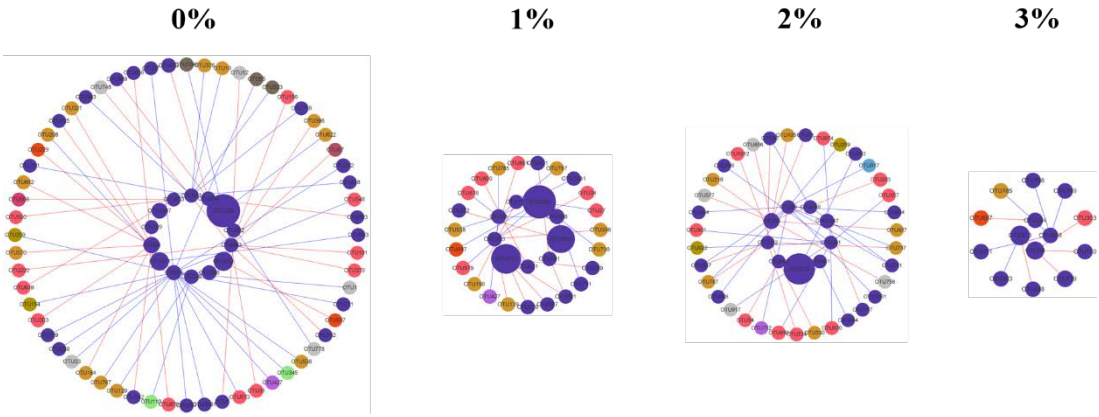

Fig. S4 Variation of the subnetwork interactions of denitrifier *Defluviicoccus* under different salinities. (Referred to the Fig. 5 for interpretation of the color in this Fig. legend).

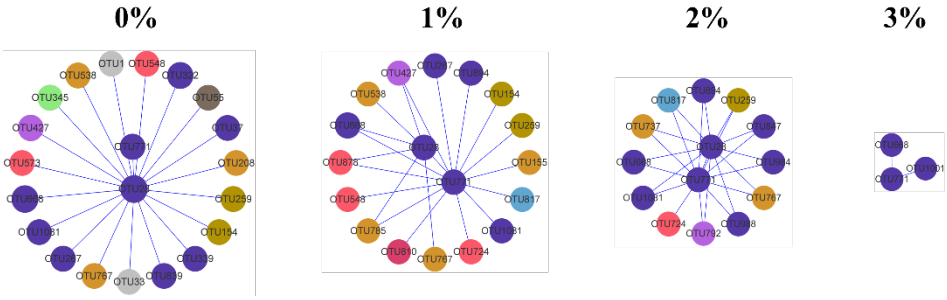

Fig. S5 Variation of the subnetwork interactions of OTUs 28 and 771 under different salinities. (Referred to the Fig. 5 for interpretation of the color in this Fig. legend).

References

Clauset A, Newman M E, Moore C (2004). Finding community structure in very large networks. Physical Review E: Statistical, Nonlinear, and Soft Matter Physics, 70(6): 066111

Deng Y, Zhang P, Qin Y, Tu Q, Yang Y, He Z, Schadt C W, Zhou J (2016). Network succession reveals the importance of competition in response to emulsified vegetable oil amendment for uranium bioremediation. Environmental Microbiology, 18(1): 205–218

Luo F, Zhong J, Yang Y, Scheuermann R H, Zhou J (2006). Application of random matrix theory to biological networks. Physics Letters. [Part A], 357(6): 420–423

Luo F, Yang Y, Zhong J, Gao H, Khan L, Thompson D K, Zhou J (2007). Constructing gene co-expression networks and predicting functions of unknown genes by random matrix theory. BMC Bioinformatics, 8: 299

Maslov S, Sneppen K (2002). Specificity and stability in topology of protein networks. Science, 296(5569): 910–913

Tu Q, Yuan M, He Z, Deng Y, Xue K, Wu L, Hobbie S E, Reich P B, Zhou J (2015). Fungal communities respond to long-term CO_2 elevation by community reassembly. Applied and Environmental Microbiology, 81(7): 2445–2454

Zhou J, Deng Y, Luo F, He Z, Tu Q, Zhi X (2010). Functional molecular ecological networks. mBio, 1(4): e00169–10